GEOPHYSICAL RESEARCH LETTERS, VOL. 21, NO. 15, PAGES 1663-1666, JULY 15, 1994

DSM complete synthetic seismograms: P-SV, spherically symmetric, case

Phil R. Cummins

Research School of Earth Sciences, Australian National University, Canberra, Australia

Robert J. Geller and Nozomu Takeuchi

Department of Earth and Planetary Physics, Faculty of Science, Tokyo University, Tokyo, Japan

Abstract. In a previous paper, [*Cummins et al.*, 1994, hereafter referred to as DSMI], we presented theoretical and computational results for calculating complete SH (toroidal) synthetic seismograms for spherically symmetric, isotropic, media. We now extend our treatment to the P-SV (spheroidal) part of the wavefield. No asymptotic approximations are used, and the synthetics, which include both body and surface waves, can be computed for a broad range of frequencies. Examples of synthetic profiles are presented for a 600km deep source in the IASP91 model for the period range 4-5000s. Such synthetics can contribute greatly to the determination of earth structure from analyses of broadband seismograms.

Theory

Following the general DSM (Direct Solution Method) treatment for a fluid-solid medium [*Geller and Ohminato*, 1994, hereafter referred to as GO], the dependent variable in the fluid part of the medium is a scalar which is proportional to pressure, while the dependent variable in the solid part of the medium is the displacement. Continuity of displacement and traction at the fluid-solid boundaries is enforced by an additional matrix operator. The Earth's self-gravitation and rotation are not included in our calculations.

As in DSMI, we use lower case roman subscripts i, j, k, to denote cartesian vector components, and subscripts r, θ, ϕ, to denote the components of vectors in spherical coordinates. Greek subscripts and superscripts (e.g., $\alpha \rightarrow (k,\ell,m,p)$) refer to the abstract vector space of trial functions, where k, ℓ, m, and $p = 1$ or 2 correspond to the radial trial function, the angular order, the azimuthal order, and the vector spherical harmonic ($\mathbf{S}^1$ or $\mathbf{S}^2$), respectively.

We use vector trial functions $\mathbf{\Phi}^{(\alpha)}$ to represent the displacement in the solid part of the medium, and scalar trial functions $\Phi^{(\alpha)}$ to represent the dependent variable, $Q = P/\omega$, where P is the change in the pressure, in the fluid part of the medium:

$$\mathbf{u} = \sum_{\alpha} c_\alpha \mathbf{\Phi}^{(\alpha)} \ , \ Q = \sum_{\alpha} c_\alpha \Phi^{(\alpha)}. \tag{1}$$

For the scalar trial functions α is a pointer to the triplet of indices ($\alpha \rightarrow (k,\ell,m)$).

The vector trial functions in the solid are

$$\begin{aligned} \mathbf{\Phi}^{(k\ell m1)} &= X_k(r)\,(Y_{\ell m}\,,0,0) \\ \mathbf{\Phi}^{(k\ell m2)} &= \frac{X_k(r)}{L}\left(0, \frac{\partial Y_{\ell m}}{\partial \theta}, \frac{1}{\sin\theta}\frac{\partial Y_{\ell m}}{\partial \phi}\right), \end{aligned} \tag{2}$$

while the scalar trial functions in the fluid regions are:

$$\Phi^{(k\ell m)} = X_k(r) Y_{\ell m}. \tag{3}$$

$Y_{\ell m}(\theta,\phi)$ is a (fully normalized) surface spherical harmonic [e.g., *Press et al.*, 1986, p.181] of angular order ℓ and azimuthal order m, k is the index for the radial dependence of the basis functions, and $L = \sqrt{\ell(\ell+1)}$.

We choose linear splines as the radially dependent part of the trial functions. Their explicit form is

$$X_k(r) = \begin{cases} (r - r_{k-1})/(r_k - r_{k-1}) & r_{k-1} < r \le r_k \\ (r_{k+1} - r)/(r_{k+1} - r_k) & r_k \le r < r_{k+1} \\ 0 & \text{otherwise,} \end{cases} \tag{4}$$

where $r_1 < r_2 \cdots < r_N$. For each distinct region (e.g., the inner core, outer core, and mantle), the second line in (4) is ignored for the uppermost layer, while the first line in (4) is ignored for the lowermost layer.

Due to the degeneracy of the problem, the matrix elements depend only on ℓ and are independent of m. The following discussion therefore considers the matrix elements and DSM equation of motion for some particular ℓ and m; for simplicity we henceforth omit the indices ℓ and m. We thus denote the elements of the matrices as $T_{k'p',kp}$ and $H_{k'p',kp}$ for the solid part of the medium, and $T_{kk'}$ and $H_{kk'}$ for the fluid part of the medium.

For a spherically symmetric fluid-solid medium the DSM equation of motion is (GO, Section 4):

$$(\omega^2\mathbf{T} - \mathbf{H} + \omega\mathbf{R})\mathbf{c} = -\mathbf{g}. \tag{5}$$

The matrix $\mathbf{R}$ enforces continuity of displacement and traction at fluid-solid boundaries.

We define the following intermediate integrals for the solid part of the medium:

Paper number 94GL01281
0094-8534/94/94GL-01281$03.00

$$
\begin{aligned}
I^0_{k'k} &= \int \rho r^2 X_{k'} X_k dr \quad & I^1_{k'k} &= \int \lambda X_{k'} X_k dr \\
I^2_{k'k} &= \int \lambda r X_{k'} \dot{X}_k dr & I^3_{k'k} &= \int \lambda r^2 \dot{X}_{k'} \dot{X}_k dr \\
I^4_{k'k} &= \int \mu X_{k'} X_k dr & I^5_{k'k} &= \int \mu r \dot{X}_{k'} X_k dr \\
I^6_{k'k} &= \int \mu r^2 \dot{X}_{k'} \dot{X}_k dr \quad ,
\end{aligned} \tag{6}
$$

where the dot denotes differentiation with respect to r. The integrals in (6) and (9), below, are non-zero only if $|k - k'| \leq 1$.

Using the above intermediate expressions, the matrix elements for the solid part of the medium are

$$
\begin{aligned}
T_{k'1,k1} &= T_{k'2,k2} = I^0_{k'k} \\
T_{k'1,k2} &= T_{k'2,k1} = 0
\end{aligned} \tag{7}
$$

and

$$
\begin{aligned}
H_{k'1,k1} &= 4I^1_{k'k} + 2(I^2_{k'k} + I^2_{kk'}) \\
&\quad + I^3_{k'k} + (L^2+4) I^4_{k'k} + 2I^6_{k'k} \\
H_{k'2,k2} &= L^2 I^1_{k'k} + (2L^2 - 1) I^4_{k'k} \\
&\quad - (I^5_{k'k} + I^5_{kk'}) + I^6_{k'k} \\
H_{k'1,k2} &= -L(2I^1_{k'k} + I^2_{kk'} + 3I^4_{k'k} - I^5_{kk'}) \\
H_{k'2,k1} &= -L(2I^1_{k'k} + I^2_{k'k} + 3I^4_{k'k} - I^5_{k'k}).
\end{aligned} \tag{8}
$$

The rows and columns of the portions of the matrices corresponding to the solid are ordered with p changing most rapidly (see Table A3 of GO). This leads to both $\mathbf{H}$ and $\mathbf{T}$ being block tridiagonal, with each block having dimension 2×2 (Figure 1).

We define the following intermediate integrals for the fluid part of the medium:

$$
\begin{aligned}
I^{F0}_{k'k} &= \int r^2 X_{k'} X_k / \lambda \, dr \quad & I^{F1}_{k'k} &= \int X_{k'} X_k / \rho \, dr \\
I^{F2}_{k'k} &= \int r^2 \dot{X}_{k'} \dot{X}_k / \rho \, dr \quad .
\end{aligned} \tag{9}
$$

The matrix elements for the fluid part of the medium are

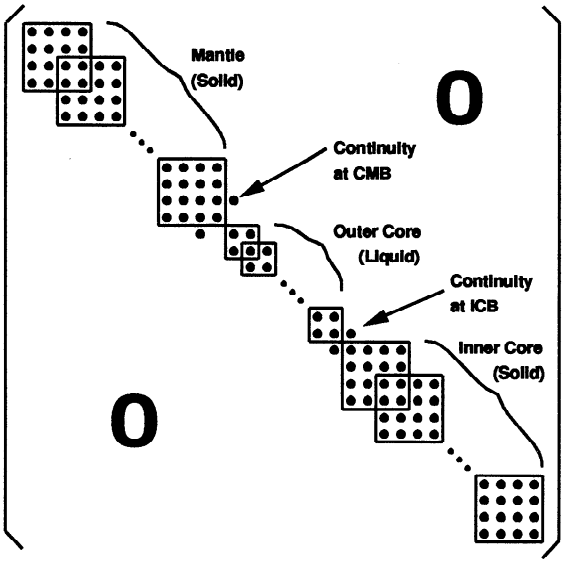

Figure 1. Structure of $\omega^2 \mathbf{T} - \mathbf{H} + \omega \mathbf{R}$.

$$
T_{k'k} = I^{F0}_{k'k} \quad , \quad H_{k'k} = L^2 I^{F1}_{k'k} + I^{F2}_{k'k}. \tag{10}
$$

Note that $\mathbf{T}$ and $\mathbf{H}$ are tridiagonal matrices for the fluid part of the medium.

At the boundary between the solid and fluid media there are two nodes corresponding to the same depth. At the ICB (Inner Core Boundary) the indices for these nodes are k^-_{ICB} for the solid medium and k^+_{ICB} for the fluid, while for the CMB (Core-Mantle Boundary) we have k^-_{CMB} for the fluid and k^+_{CMB} for the solid. As shown by GO (eqs. 50-51) $\mathbf{R}$ enforces the continuity of displacement and traction at fluid-solid boundaries. The only non-zero elements of $\mathbf{R}$ are:

$$
\begin{aligned}
R_{k^-_{ICB}1, k^+_{ICB}} &= R_{k^+_{ICB}, k^-_{ICB}1} = r^2_{ICB} \\
R_{k^-_{CMB}1, k^+_{CMB}} &= R_{k^+_{CMB}, k^-_{CMB}1} = -r^2_{CMB},
\end{aligned} \tag{11}
$$

where r_{ICB} and r_{CMB} are the radius at the ICB and CMB respectively. Extending the above results to a medium with more than one fluid region is straightforward. The essential boundary condition $u_r = u_\theta = u_\phi = 0$ is imposed at $r = 0$.

Excitation

The displacement scalars $U(r)$ and $V(r)$ in the solid parts of the medium (sometimes denoted by y^S_1 and y^S_3 respectively) are defined as follows:

$$
U(r) = \sum_k c_{k1} X_k(r) \qquad V(r) = \sum_k c_{k2} X_k(r). \tag{12}
$$

In this section we assume the source is a point source at a node in the mantle. The body force equivalent for a point moment tensor is sometimes kinematically equivalent to requiring the displacement scalars to be discontinuous at the source depth $r = r_s$. Since the definition of $U(r)$ and $V(r)$ in (12) forces them to be continuous (as they are a superposition of continuous trial functions), convergence of the DSM solution of (5) for this case is suboptimal. We therefore directly incorporate the discontinuity into the definition of $U(r)$ and $V(r)$ in a manner analogous to that used in DSMI for $W(r)$. For a point moment tensor on the z-axis ($r = r_s$, $\phi = 0$, $\theta \to 0$), the discontinuity in U and V is given by [*Takeuchi and Saito*, 1972, p. 289]

$$
\begin{aligned}
D_1 &= U(r)\big|^{r_s^+}_{r_s^-} = b_1 \delta_{m0} 2M_{rr} / [r_s^2 (\lambda_s + 2\mu_s)] \\
D_2 &= V(r)\big|^{r_s^+}_{r_s^-} = b_1 \delta_{m\pm1} (\mp M_{r\theta} + i M_{r\phi}) / [r_s^2 \mu_s]
\end{aligned} \tag{13}
$$

where $\lambda_s = \lambda(r_s)$, $\mu_s = \mu(r_s)$, and $b_1 = ((2\ell + 1)/16\pi)^{1/2}$. We define continuous functions U' and V',

$$
U'(r) = U(r) - D_1 H(r - r_s) \tag{14}
$$

$$
V'(r) = V(r) - D_2 H(r - r_s), \tag{15}
$$

where $H(r - r_s)$ is a Heaviside step function. We expand U' and V' in terms of the trial functions.

$$
U'(r) = \sum_k c'_{k1} X_k(r) \qquad V'(r) = \sum_k c'_{k2} X_k(r). \tag{16}
$$

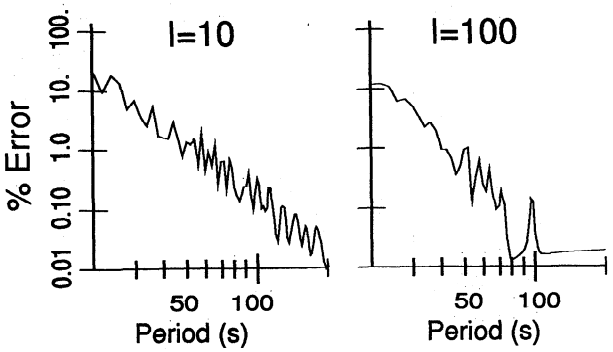

Figure 2. Error of DSM solutions.

We now define a matrix

$$\mathbf{A} = \omega^2 \mathbf{T}' - \mathbf{H}', \tag{17}$$

where $\mathbf{T}'$ and $\mathbf{H}'$ are defined in the same way as $\mathbf{T}$ and $\mathbf{H}$ in (7) and (8), except that the integrals in (6) are evaluated only from r_s to the earth's surface. (Note that we are assuming the source is in the mantle.) We next define

$$g'_{kp} = \sum_{k'p'} D_{p'} A_{kp,k'p'} \tag{18}$$

We then find the expansion coefficients for $\mathbf{c}'$ by solving

$$(\omega^2 \mathbf{T} - \mathbf{H} - \omega \mathbf{R})\mathbf{c}' = -\mathbf{g}' \tag{19}$$

Finally, having found $\mathbf{c}'$, we use (14) and (15) to find U and V.

In contrast, for the remaining elements of the moment tensor, U and V are continuous at $r = r_s$, but the tractions (y_2^S and y_4^S) are discontinuous. We find $\mathbf{c}$ for these cases by solving by eq. (5) using the following force vector:

$$\begin{aligned} g_{k1} &= b_1 \delta_{m0} 2(M_{\theta\theta} + M_{\phi\phi} \\ &\quad - M_{rr} 2\lambda_s/(\lambda_s + 2\mu_s))[U_k(r)/r]_{r=r_s} \\ g_{k2} &= b_1 \delta_{m0} L(-M_{\theta\theta} - M_{\phi\phi} \\ &\quad + M_{rr} 2\lambda_s/(\lambda_s + 2\mu_s))[V_k(r)/r]_{r=r_s} \\ &\quad - b_2 \delta_{m\pm 2}(M_{\phi\phi} - M_{\theta\theta} \\ &\quad \pm i 2 M_{\theta\phi})[V_k(r)/r]_{r=r_s} \end{aligned} \tag{20}$$

where $b_2 = ((2\ell+1)(\ell-1)(\ell+2)/(64\pi))^{1/2}$.

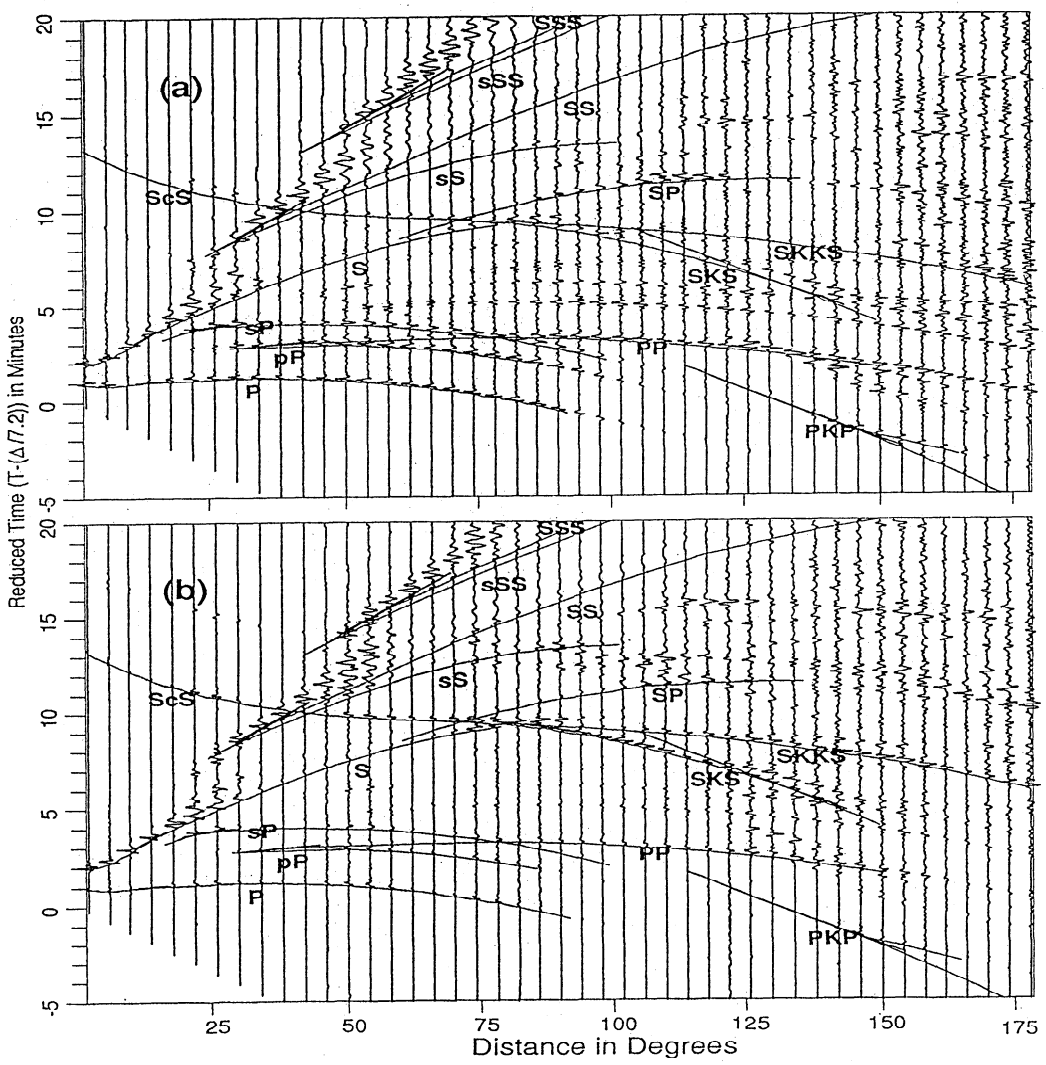

Figure 3. (a) Synthetic vertical (r) component record section for a 600 km deep source for the IASP91 model. (b) Same as (a), except that the synthetics are for radial (θ) component seismograms.

Numerical Example

The Earth model used is IASP91 [*Kennett and Engdahl*, 1991], with density and Q structure based on PREM [*Dziewonski and Anderson*, 1981]. Physical dispersion is included. The point moment tensor source has a δ-function time history and corresponds to slip along a horizontal fault in the $\phi = 0$ direction. The source is at a node at 600 km depth, and the number of layers in the inner core, outer core, and mantle are 350, 600, and 800, respectively.

The error of the DSM solutions decreases with increasing period for a fixed layer thickness. This is illustrated in Figure 2, which shows the error of the DSM solutions (obtained by comparison to solutions obtained by numerical integration of the strong form of the equation of motion [*Takeuchi and Saito*, 1972]).

Figure 3(a, b) shows record sections of r- and θ- component (i.e., vertical and radial) synthetic seismograms for the above Earth model and source. The synthetics are computed for a receiver profile in the $\phi = 0°$ direction. A low-pass filter with a corner frequency of 0.125 Hz is used to avoid a sharp cut-off at the 0.25 Hz Nyquist frequency.

The arrival times of major body-wave phases from ray-theoretical travel time curves [*Sambridge and Kennett*, 1990] are superposed on the record sections. These arrival times agree extremely well with the body-wave arrivals. The direct P and S waves, as well as boundary interaction phases (SS, SSS, ScS) and converted waves (SP, SKS) arrive at the times predicted for model IASP91. Note in particular the PKP triplication near 150°, which involves phases travelling through the inner and outer cores.

Shear-coupled PL is prominent in Figures 3a and 3b. This is a long period, dispersive wave train which emerges just after S, SS, and SSS [e.g., *Oliver and Major*, 1960; and *Poupinet and Wright*, 1981]. It is excited due to the coupling of an S body wave (S, SS, or SSS) incident on the crust from below to the fundamental leaking mode of Rayleigh waves in the crustal waveguide [*Baag and Langston*, 1985].

The calculation, which is not yet fully optimized, was carried to a Nyquist frequency of 0.25 Hz, and required about 300 hr on a Sparc-10 workstation. The CPU time required for a Nyquist frequency of 50 mHz (a Nyquist period of 20s) was about 5 hr.

Acknowledgments. We thank Malcolm Sambridge for use of his ray-tracing program, and the Japan Society for the Promotion of Science for the support provided to P.R.C. and N.T. for part of this work. This research was partially supported by a grant from the Japanese Ministry of Education, Science and Culture (No. 06640542) and by the ISM Cooperative Research Program (94-ISM-CRP-53).

References

Baag, C.-E., and C. A. Langston, Shear-coupled PL, *Geophys. J. R. Astron. Soc., 80*, 363-385, 1985.

Cummins, P. R., R. J. Geller, T. Hatori, and N. Takeuchi, DSM complete synthetic seismograms: SH, spherically symmetric, case, *Geophys. Res. Lett., 21*, 533-536, 1994.

Dziewonski, A. M., and D. L. Anderson, Preliminary Reference Earth Model, *Phys. Earth Planet. Inter., 25*, 297-356, 1981.

Geller, R. J., and T. Ohminato, Computation of synthetic seismograms and their partial derivatives for heterogeneous media with arbitrary natural boundary conditions using the Direct Solution Method, *Geophys. J. Int., 116*, 421-446, 1994.

Kennett, B. L. N., and E. R. Engdahl, Traveltimes for global earthquake location and phase identification, *Geophys. J. Int., 105*, 429-465, 1991.

Oliver, J., and M. Major, Leaking modes and the PL phase, *Bull. Seismol. Soc. Am., 50*, 165-180, 1960.

Poupinet, G., and C. Wright, The generation and properties of shear-coupled PL waves, *Bull. Seismol. Soc. Am., 62*, 1699-1710, 1972.

Press, W. H., B. P. Flannery, S. A. Teukolsky, and W. T. Vetterling, *Numerical Recipes*, Cambridge U. Press, 818pp, 1986.

Sambridge, M. S., and B. L. N. Kennett, Boundary value ray tracing in a heterogeneous medium: a simple and versatile algorithm, *Geophys. J. Int., 101*, 157-168, 1990

Takeuchi, H., and M. Saito, Seismic surface waves, *Meth. Comp. Phys., 11*, 217-295, 1972.

P. R. Cummins, Research School of Earth Sciences, Australian National University, GPO Box 4, Canberra ACT 0200, Australia. (e-mail: phil@rses.anu.edu.au)

R. J. Geller, and N. Takeuchi, Dept. of Earth and Planetary Physics, Faculty of Science, Tokyo University, Yayoi 2-11-16, Bunkyo-ku, Tokyo 113, Japan. (e-mail: [bob,takeuchi]@global.geoph.s.u-tokyo.ac.jp)

(received April 15, 1994;
accepted May 09, 1994.)